UCRL-JRNL-205155

Laboratory Measurements of Velocity and Attenuation in Sediments

M. Prasad, M. A. Zimmer, P. A. Berge, and B. P. Bonner

July, 2004

Society of Exploration Geophysicists, Tulsa

UCRL-JRNL-205155

DISCLAIMER

This document was prepared as an account of work sponsored by an agency of the United States Government. Neither the United States Government nor the University of California nor any of their employees, makes any warranty, express or implied, or assumes any legal liability or responsibility for the accuracy, completeness, or usefulness of any information, apparatus, product, or process disclosed, or represents that its use would not infringe privately owned rights. Reference herein to any specific commercial product, process, or service by trade name, trademark, manufacturer, or otherwise, does not necessarily constitute or imply its endorsement, recommendation, or favoring by the United States Government or the University of California. The views and opinions of authors expressed herein do not necessarily state or reflect those of the United States Government or the University of California, and shall not be used for advertising or product endorsement purposes.

This work was performed under the auspices of the U.S. Department of Energy by University of California, Lawrence Livermore National Laboratory under Contract W-7405-Eng-48.

Laboratory measurements of velocity and attenuation in sediments

M. Prasad[1], M. A. Zimmer[1], P. A. Berge[2], and B. P. Bonner[2]
[1]Geophysics Department, Stanford University, Stanford, CA 94305. E-mail: manika.prasad@stanford.edu, zimmer@pangea.stanford.edu.
[2]Earth Science Division, Lawrence Livermore National Laboratory, 7000 East Ave., Livermore, CA 94550. E-mail: bonner1@llnl.gov, berge1@llnl.gov.

ABSTRACT

Laboratory measurements are required to establish relationships between the physical properties of unconsolidated sediments and P- and S-wave propagation through them. Previous work has either focused on measurements of compressional wave properties at depths greater than 500 m for oil industry applications or on measurements of dynamic shear properties at pressures corresponding to depths of less than 50 m for geotechnical applications. Therefore, the effects of lithology, fluid saturation, and compaction on impedance and P- and S-wave velocities of shallow soils are largely unknown. We describe two state–of–the–art laboratory experiments. One setup allows us to measure ultrasonic P-wave velocities at very low pressures in unconsolidated sediments (up to 0.1 MPa). The other experiment allows P- and S-wave velocity measurements at low to medium pressures (up to 20 MPa). We summarize the main velocity and attenuation results on sands and sand – clay mixtures under partially saturated and fully saturated conditions in two ranges of pressures (0 – 0.1 MPa and 0.1 – 20 MPa) representative of the top few meters and the top 1 km, respectively. Under hydrostatic pressures of 0.1 to 20 MPa, our measurements demonstrate a P- and S-wave velocity-dependence in dry sands around a fourth root (0.23 –0.26) with the pressure dependence for S-waves being slightly lower. The P- velocity-dependence in wet sands lies around 0.4. The Vp-Vs and the Qp-Qs ratios together can be useful tools to distinguish between different lithologies and between pressure and saturation effects. These experimental velocities at the frequency of measurement (200 kHz) are slightly higher that Gassmann's (Gassmann, 1951) static result. For low pressures under uniaxial stress, Vp and Vs were a few hundred meters per second with velocities showing a strong dependence on packing, clay content, and microstructure. We provide a typical shallow soil scenario in a clean sand environment and reconstruct the velocity profile of such a sediment packet.

INTRODUCTION

Seismic velocities and attenuations collected in the field with, for example, reflection, refraction, and cross-hole surveys serve as valuable constraints on subsurface lithology, porosity, permeability, and fluid saturation. Until recently, the measurement resolution of seismic velocities in the shallow subsurface had limited the use of the complete power of seismic attribute analysis in shallow soils. Recent advances in field techniques for seismic measurements in shallow soils (e.g., Bachrach et al., 1998, 2002 (this volume); Baker et al., 1999; Carr et al., 1998; Steeples et al., 1999) as well as the development of seismic cone penetration tests (SCPT) and other improved geotechnical methods (e.g., Crouse et al., 1993; Boulanger et al., 1998) have begun to permit the application of seismic attribute analysis to shallow soils. Unfortunately, the laboratory studies required for establishing relations between the physical properties of the soils and their seismic properties have not been extended to the low pressures analogous to these shallow depths, so the effects of lithology, fluid saturation, and compaction on seismic (P- and S-wave) properties of shallow soils are largely unknown.

Interpretation of shallow seismic data requires knowledge about P- and, to a lesser extent, S-wave propagation in sediments at low pressures. A wealth of geotechnical literature exists in measurements of shear modulus at low pressures (e.g., Santamarina et al., 2001). Often, these measurements lack P-wave information, which is crucial for field seismic studies. In geophysical literature, the focus has been mainly for oil industry application. Thus, the effects of physical properties and fluid content on the seismic properties of sedimentary rocks have been studied extensively at higher pressures using ultrasonic measurements and other laboratory techniques (e.g., Domenico, 1976; Cheng, 1978; Han et al., 1986; Wilkens et al., 1986; Knight and Nolen-Hoeksema, 1990; Vernik and Nur, 1992; Green et al., 1993; Prasad and Manghnani, 1997). Interpretation methods in common use for seismic field data have been developed for oil industry applications (e.g., Wyllie et al., 1956; Kuster and Toksöz, 1974). They are not optimized for the shallow depths and unconsolidated materials of environmental or engineering applications. P- and S-wave laboratory data collected for soils at low-pressure conditions appropriate to the near surface are sparse in the literature. Although laboratory data sets are available in the exploration geophysics, marine geophysics, and soil mechanics literature (e.g., Rao, 1966; Domaschuk and Wade, 1969; Domenico, 1976; Hamilton and Bachman, 1982; Prasad and Meissner, 1992; Santamarina et al., 2001), few studies

(Hamilton and Bachman, 1982; Zimmer et al., 2000; 2002a; Prasad, 2002) include both compressional and shear wave velocity measurements as a function of pressure at the extremely low pressures representing the shallow subsurface. Relevant laboratory measurements of soil properties will enable us to develop new interpretation techniques for seismic field data for environmental and engineering applications.

To this end, we describe state–of–the–art laboratory experiments involving the measurement of ultrasonic velocities at low pressures in unconsolidated sediments and summarize the main velocity results. The on-going experiments at Stanford University and Lawrence Livermore National Laboratory (LLNL) were developed to make accurate measurements of compressional-wave (Vp, Qp) and shear-wave (Vs, Qs) velocities and attenuations in highly-attenuating soils at low pressures (e.g., Aracne-Ruddle et al., 1998; 1999; Bonner et al., 1999a, 2000, 2001; Zimmer et al., 2002a; 2002b; Prasad, 2002). The data presented here include LLNL uniaxial measurements on dry, saturated, and partially-saturated sands and sand-clay mixtures made at pressures below approximately 0.1 MPa; and Stanford hydrostatic measurements made on dry and water-saturated sands at pressures from 0.1 MPa to 20 MPa. Also presented here are velocity – pressure transforms developed from the Stanford data for predicting Vp and Vs. Methods developed from the LLNL data for relating velocities to lithology are described elsewhere (for example, Bertete-Aguirre and Berge, 2002). The LLNL and Stanford ultrasonic velocity measurements for unconsolidated soils at low stresses confirm recent field observations of extremely low seismic velocities in shallow soils (e.g., Bachrach et al., 1998; Carr et al., 1998; Steeples et al., 1999). These experimental results should allow for the development of empirical and theoretical models that will permit more accurate inversions of shallow seismic data for the physical properties and fluid content of soft soils (e.g., Bertete-Aguirre and Berge, 2002; Berge and Bonner, 2002). Such seismic interpretation methods can help guide effective in situ environmental remediation and foundation engineering.

EXPERIMENTAL METHODS

Laboratory experiments under well-controlled conditions allow us to understand the physics of wave propagation in sediments and to develop predictive empirical relations. It has been standard geophysical laboratory practice to conduct such experiments on rocks typically at 1 MHz frequency under high confining pressures. Considerable design is

required to modify such experiments to overcome experimental challenges and simulate shallow soil conditions in the laboratory. For example,

1. Very low pressures must be maintained in experiments to simulate the in situ conditions of shallow soils.
2. Experimental design should avoid impedance mismatch between standard high-impedance acoustic transmitters and low-impedance soils. Thus, the commonly used high-impedance metal transducer plates need to be replaced with plates made from low impedance materials.
3. Maintain high signal amplitude and high signal-to-noise ratio: Since unconsolidated sediments are highly attenuating, high signal energy is necessary to propagate elastic waves through them. Using lower frequencies reduces attenuation and produces a higher energy signal.

We report here two different types of equipment to simulate very low pressures and generate a high signal output to propagate through unconsolidated materials. One experiment (called the LLNL experiment) was designed to measure ultrasonic velocities in sediments at dry, fully and partially saturated conditions under uniaxial loads up to 0.1 MPa. The second experiment (called the Stanford experiment) was designed to measure velocities in sediments at dry and at fully saturated conditions under confining pressures up to 20 MPa. Special care was taken to ensure generation of interpretable signals at low pressures of 0.1 MPa.

The LLNL experimental setup

In the Experimental Geophysics Laboratory at LLNL, we used the pulse transmission technique (Sears and Bonner, 1981) to measure ultrasonic compressional and shear wave velocities for dry and fully saturated sediments. We also measured velocities in sand samples with various degrees of partial saturation (Bonner et al., 2001).

Measurements were made on 4.49 cm long cylinders with 4.7 cm diameter at room temperature and at pressures between about 0.01 and about 0.1 MPa to simulate the top few meters of the subsurface. In order to obtain good ultrasonic signals at these low pressures, the transmitting transducer was driven with unusually high voltages, approaching the dielectric breakdown. The transducers were also operated at frequencies at the low end of the available range, from about 100 to 500 kHz. A low noise, high-gain preamplifier was needed and extensive signal averaging was used to improve the signal-to-noise ratio. High-insertion-loss sample containers were required to suppress arrivals

that travel around the sample to obscure true arrivals, to make it possible to detect shear waves in unconsolidated samples at low pressures. The sample containers provided over 100 dB insertion loss to control leakage of ultrasound, by using geometric constraints to suppress low frequencies and material selection to attenuate high frequencies (Bonner et al., 1999b). The sample assemblies were closed with latex membranes that transmitted sound from the transducer and contained the soil mixture. Accuracy (= repeatability of measurements) was limited to 20% at the lowest stresses near 1 psi (0.007 MPa), but improved with signal amplitude to about 3% for compressional (P) waves and 10% for shear (S) waves at higher stresses. Precision in timing the arrivals (= uncertainity of first arrival picks) was about 1% for P and 2 to 5% for S arrivals in most cases. Sample length change was less than 0.1% at the highest pressures and thus was considered negligible. Details of the experimental procedures are given in Aracne-Ruddle et al. (1999).

Up to several meters of overburden were simulated by applying low uniaxial stress up to about 0.1 MPa to the sample using a pneumatic system. Although the sample sleeve was not perfectly rigid, the internal stress in the sample approximately corresponded to the uniaxial strain condition. Pore fluid pressures, applied using a regulated gas tank (Figure 1), could be increased beyond the sample bubble pressure to expel water and produce partial saturation. Tensiometers were used to measure the pressure in the continuous aqueous phase when the sample was partially saturated. The difference between applied and water-phase pressure is the capillary pressure. Results of LLNL measurements for some samples are presented later in this chapter.

The Stanford experimental setup

The apparatus developed in the Rock Physics Laboratory at Stanford University used pulse transmission to measure the ultrasonic P and S velocities and attenuations of unconsolidated sands at hydrostatic pressures from 100 kPa to 20 MPa. Zimmer et al. (2000; 2002a) have described details of the experimental setup; the main features are given here. The apparatus consists of a sample holder (Figure 2a) that is placed into a pressure vessel (Figure 2b) capable of producing confining pressures of up to 20 MPa. The samples are 3.8 cm in diameter and about 3 cm in length. The sample holder consists of two end caps that contain the ultrasonic transducers and that are supported in a steel frame. The transducers were constructed with lower (200 kHz) than traditional ultrasonic

(1 MHz) frequency piezoelectric crystals and with low-impedance face plates made out of a glass-filled polycarbonate in order to maximize the elastic wave energy propagated through the sample. The sample holder was also designed to be disassembled and reassembled easily, and can be placed in the pressure vessel with minimal disturbance. These features were necessary in order to permit consistent sample preparation so as not to obscure the effects of the textural variations of the sands on the ultrasonic measurements. With this arrangement we were able to get interpretable shear wave signals through saturated samples at pressures as low as 100 kPa. An error analysis that took into account errors in the length measurements, the measurement of the delay times, and ambiguities in the pick of arrival times gave error estimates of about 2% for the Vp values, and about 4% for the Vs values over the entire pressure range (Zimmer et al., 2002a).

The static strain on the sample was registered using three axial gauges that measured the length change between the end caps and one circumferential gauge that measured the change in the circumference of the middle of the sample. The axial measurements allowed us to determine accurately the length of the sample and to detect any tilting of the end caps relative to each other. The circumferential gauge allowed us to make better estimates of the volume and porosity of the sample, as it told us how much the sample deviated from a purely cylindrical shape.

The next section of this paper describes some of the LLNL and Stanford samples, and following sections summarize and discuss some measurement results.

SAMPLES

The sediments used in both the LLNL and the Stanford experiments were made artificially in order to study the relations between sediment texture (that is, porosity, composition, and compaction) and its seismic properties under well-defined and reproducible conditions. In the LLNL experiments, sand and sand-clay mixtures were measured. The Stanford experiments were made on natural sands. Both experiments were first made to understand the physical processes in sediments. Future research will concentrate on effects of fabric differences between artificial samples and natural soils.

LLNL sand-clay and sand samples

The artificial sediment samples that LLNL made were fabricated from Ottawa sand mixed with a swelling clay. The sand comes from a quarry near the city of Ottawa, Illinois and is Middle Ordovician in age. It is composed entirely of well-rounded quartz grains (Domenico, 1976). The sand was sieved to a median grain diameter of 273 μm, with grain sizes ranging from 74 to 420 μm. The clay was Wyoming bentonite, a sodium montmorillonite from Wyoming that is a swelling smectite. The clay was equilibrated in a 100% humid atmosphere for seven days before sample preparation, in order to achieve reproducible water content. The clay content in the sand-clay samples was 1 to 40 percent by mass. Bulk density ranged from about 1400 to 1700 kg/m^3, where the lowest density corresponded to the sample having 40% clay by mass and pure sand samples had densities of about 1700 kg/m^3. We found that the packing affected measured velocities and their load dependence. We were able to achieve reproducible results using a hand-held brass weight that fit snugly in the sample holder. Sample preparation and composition are discussed in detail in Aracne-Ruddle et al. (1999) and Bonner et al. (2001).

Stanford sand samples for hydrostatic experiments

The measurements collected with the hydrostatic apparatus at Stanford were all made on samples of the Santa Cruz aggregate, a fine-grained, well-sorted, angular quartz sand from Santa Cruz, California. We prepared water-saturated samples first sliding the jacket over the lower end cap and then filling it with water. The sand was then poured slowly into the water and was stirred slightly to allow any air bubbles to escape and to level off the top of the sample. The upper end cap was then slid into the jacket above the sample until it just rested on the top of the sand, so the sand was not pre-compacted. The sample holder was then assembled and placed into the pressure vessel. To ensure repeatability and yet maintain high initial porosity, dry samples were prepared by air pluviating the sand into the jacket, and then leveling off the top by placing a 160 g aluminum weight on top of the sand about 20 times.

Once the sample holder was placed in the pressure vessel, measurements were made at regular pressure steps as the pressure was cycled through one to five pressure cycles, with each cycle peaking at a slightly higher pressure up to 20 MPa. The measurement results from two water-saturated sand samples and two dry sand samples are presented in the results section of this paper. Typical waveforms for P- and S-waves in a sand sample at two pressures (0.05 and 20 MPa) are shown in Figures 3a – d.

RESULTS

Vp and Vs results for sands and sand-clay mixtures from the LLNL experiments

Figures 4a and 4b present LLNL results for Vp and Vs with respect to pressure for dry sands and sand-clay mixtures. The pressures are equivalent to about the top 5 m of the subsurface. Differences in packing and clay content control the measured velocities. Figure 4c shows velocities vs. clay content for samples packed in the same way, for measurements made at about 0.1 MPa. Clay content is shown schematically below the plot in Figure 4c. We see in Figure 4c that although Vs decreases monotonically with increasing clay content, Vp initially increases as clay causes sand grains to stick together and fills dry pores. Then, Vp decreases with increasing clay content when the amount of clay is enough to form a continuous clay matrix through the sample. Similar behavior has been observed for sand-clay mixtures at 10 to 50 MPa (Marion et al., 1992). Vs does not show the same behavior. Apparently, the clay does not impede sliding between grains.

Table 1 shows velocity as a function of saturation for Ottawa sand samples. The water content was obtained from the water retention curve (Bonner et al., 2001). Velocity results and related uncertainties are described in detail elsewhere (Bonner et al., 1997, 1999a, 2000, 2001; Aracne-Ruddle et al., 1998, 1999; Berge et al., 1999). Our main findings are that the microstructure controls the velocities; the velocities are low, a few hundred m/s in dry samples, with Vp values being about twice the Vs values; velocities and amplitudes depend on the amount and distribution of fluid in saturated and drained samples; and the velocity gradients at the lowest pressures are strongly influenced by grain packing (Figure 4). Comparison of our laboratory velocity results to available

seismic reflection and refraction data (e.g., Crouse et al., 1993; Taylor and Wilson, 1997; Bachrach et al., 1998; Boulanger et al., 1998; Steeples et al., 1999) showed agreement between velocities measured in the lab and field for soils of similar types, at lab pressures equivalent to the appropriate depth for the field measurements.

Vp and Vs results for sands from the Stanford experiments

Figure 5 shows the Vp and Vs results for four samples of the Santa Cruz aggregate tested in the Stanford hydrostatic apparatus. Details of our results are described in Zimmer et al. (2002a; 2002b). The most important point relevant to shallow seismic applications is that the velocity – pressure dependence can be described for the S-waves by a fourth-root relation over the entire pressure range from 100 kPa to 20 MPa, while the P-wave dependence is closer to a fifth root dependence. The velocity data are very consistent between different samples and between different pressure cycles for the same sample. They also agree well with similar sand data from Domenico (1976), Prasad and Meissner (1992), Yin (1992), and Robertson et al. (1995). Solid lines in Figure 5 represent empirical fits to the data.

Empirical fits to the velocity data in Figure 5 are of the form

$$V = a + bP^c \qquad (1)$$

where V is the velocity (m/s), and P is the pressure (MPa). These empirical fits demonstrate a velocity dependence to approximately the fifth root of the pressure. The exact empirical coefficients for each case are given in Table 2.

Attenuation results

As seismic waves pass through sediments and rocks, they loose energy. This attenuation or dissipation of seismic wave energy is greater in the loose sediments typical of the shallow subsurface. Since attenuation depends, among other factors on material properties, it can potentially be used to predict these properties. Futterman (1962) defines the dissipation, Q^{-1}, (inverse of quality factor, Q) as the ratio of energy loss per cycle (ΔE) to the maximum energy (E) stored in the system:

$$Q^{-1} = \frac{\Delta E}{2\Pi E} = (1 - \exp(\frac{4\Pi V_i}{V_r}))2\text{p} \ , \qquad (2)$$

where the complex velocity V = Vr + iVi.

O'Connell and Budiansky (1977) have shown that the quality factor can also be described in terms of the complex moduli as

$$Q = \frac{M_r}{M_i}, \tag{3}$$

where the complex modulus M = Mr + iMi. Thus, Qp, the P-wave quality factor is

$$Q_P = \frac{K_r + \frac{4}{3}\mu_r}{K_i + \frac{4}{3}\mu_i}, \tag{4}$$

and Qs, the S-wave quality factor is

$$Q_S = \frac{\mu_r}{\mu_i}, \tag{5}$$

where K is the complex bulk modulus and μ is the complex shear modulus. Winkler and Nur (1982) have shown that a plot of Qp/Qs versus $(Vp/Vs)^2$ allows us to differentiate between the losses in bulk (Ki/Kr) and in shear (μi/μr). Prasad and Meissner (1992) and Prasad (2002) have shown that using both P- and S-wave velocity and attenuation allows us to differentiate between grain size and saturation in sands. Figure 6 shows a plot of $(Vp/Vs)^2$ versus Qp/Qs for dry and fully water-saturated sands. The figure shows that velocity and attenuation data can be useful tools to distinguish between different lithologies and between pressure and saturation effects. Whereas, Vp is low at both low effective pressures and in gas saturated sands, Vs is unaffected by saturation state and is extremely low at low effective pressures. Thus, Vp/Vs ratio will move in different directions for the dry and the saturated cases. In addition to low Vp-Vs ratios, dry sands also have fairly high Qp/Qs values. Analyses of the main loss mechanism (Prasad and Meissner, 1992) (solid lines in Figure 6) show that the shear losses equal bulk losses in the dry sands; bulk losses are predominant in saturated sands. Increasing effective pressure decreases Qp/Qs and Vp/Vs ratios in both cases.

DISCUSSION AND RELEVANCE TO SHALLOW SEISMIC MEASUREMENTS

Field seismic studies in the past decade have shown measurements of extremely low velocities for the shallow subsurface (e.g., Crouse et al., 1993; Taylor and Wilson, 1997; Bachrach et al., 1998; Carr et al., 1998; Steeples et al., 1999). Due to an absence of rock

physics data corresponding to such sites, interpretation of sediment properties from seismic surveys has been limited to areas where ground-truth was provided by boreholes or existing geological descriptions. Added to this lack of data is the fact that most theoretical models of unconsolidated granular media fail to predict both P- and S-wave velocities realistically. Specifically, they do not predict the very low velocities and very steep gradients that are measured in the field. This breakdown of the theoretical models has lead to uncertainties in interpretations of field seismic measurements. Our laboratory measurements of ultrasonic velocities corroborate the low velocities and high gradients observed in the seismic surveys mentioned above. The agreement between laboratory and field measurements shows that theoretical models are, at best, an oversimplification of the natural case and modifications are required for accurate predictions of natural phenomena. A further consequence of the inadequacy of the velocity models arises when analyzing Poisson's ratio values. The theoretical smooth contact radius models predict Poisson's ratio values much lower than 0.1 (Winkler, 1983; Prasad and Meissner, 1992; Bachrach et al., 1998). By adding grain roughness, Palciauskas (1992) has shown that the Poisson's ratio can be as high as 0.14. Our measured Poisson's ratio in dry sands at very low pressures lies around 0.18 – 0.36. At these low pressures in the laboratory, Poisson's ratio does not depend significantly on pressure or on partial saturation. However, after addition of clay or at full saturation, Poisson's ratio values rise to about 0.4, close to fluid values. At very low pressures, velocity is strongly dependent on composition, microstructure, and pressure.

Our results of velocities in sediments can be used for characterizing physical properties of sediments from field seismic surveys. They may also be useful for site-specific modeling. For example, Bertete-Aguirre and Berge (2002) have shown that having shear velocities available as well as P-velocities significantly improves the ability to recover lithology from seismic data even when the velocity uncertainties are high.

In a simplified, typical shallow sediment environment, the vadose zone consists of dry to partially saturated sediments. Below the water table, these sediments are water saturated (e.g., Hübner et al., 1985; Robertson et al., 1995; Bachrach et al., 2002, this volume). Depth of the water table will depend on the geographic location and on climatic conditions. We consider, as an example, a typical shallow soil scenario in a clean sand environment where the water table lies at a depth of 50m. Dry and partially saturated sands lie above the water table and fully saturated sands below it. Using our experimental results, we can now reconstruct the velocity profile of such a sediment packet as shown in

Figure 7. A steep velocity gradient will be characteristic of the uppermost layer, as shown in Figure 7. The water table will be marked by strong Vp/Vs contrast. Details of composition and fabric will affect the velocities. For example, addition of clay to the sands in the dry region will decrease velocity even further. From Figure 4, addition of moderate amounts of clay increases Vp due to cementation and pore-filling effects. With larger amounts of clay, once clay becomes load-bearing, the Vp decreases. Vs, on the other hand, decreases monotonically with addition of clay. Thus, the laboratory measurements can be powerful predictive tools to interpret field seismic data from the shallow sub-surface and to construct synthetic seismograms.

CONCLUSIONS

We have shown the importance of conducting laboratory experiments at pressures relevant for the shallow depths typical for environmental geophysics. Our results on unconsolidated sediments show that in dry sands, the pressure dependence of P- and S-wave velocities can be empirically described by a fourth root (0.23 –0.26). The P-velocity-dependence in wet sands lies around 0.4. At low pressures, velocity in dry sands shows a strong increase with pressure. Poisson's ratio values are low (0.18 – 0.3) at low pressures. Addition of water or clay to sands increases the Poisson's ratio to about 0.4.

ACKNOWLEDGEMENTS

Zimmer and Prasad's work was performed under the auspices of the Department of Energy (Award No. DE-FC26-01BC15354). Zimmer was also supported by a Chevron Stanford Graduate Fellowship. Work of Bonner and Berge was performed under the auspices of the U.S. Department of Energy by the University of California Lawrence Livermore National Laboratory under contract W-7405-ENG-48 and supported specifically by the Environmental Management Science Program of the Offices of Environmental Management and Science. Any opinions, findings, conclusions, or recommendations expressed herein are those of the authors and do not necessarily reflect the views of the DOE. We thank the reviewers for their comments.

REFERENCES

Aracne-Ruddle, C., Wildenschild, D., Bonner, B., and Berge, P., 1998, Direct observation of morphology of sand-clay mixtures with implications for mechanical properties in sediments: Eos, Transactions of the American Geophysical Union, 1998 Fall Meeting Supplement, **79**, F820.

Aracne-Ruddle, C. M., Bonner, B. P., Trombino, C. N., Hardy, E. D., Berge, P. A., Boro, C. O., Wildenschild, D., Rowe, C. D., and Hart, D. J., 1999, Ultrasonic velocities in unconsolidated sand/clay mixtures at low pressures: LLNL report UCRL-JC-135621, Lawrence Livermore National Laboratory, Livermore, CA 53 pp., available at http://www.llnl.gov/tid/lof/documents/pdf/237096.pdf; also summarized in Eos, Transactions of the American Geophysical Union, Fall Meeting Supplement, Proceedings of the Fall Annual Meeting, held in San Francisco, CA, Dec. 13-17, 1999, **80**, F397.

Bachrach, R., Dvorkin, J., and Nur, A., 1998, High-resolution shallow-seismic experiments in sand, Part II: Velocities in shallow unconsolidated sand: Geophysics, **63**, 1233-1284.

Bachrach, R., Mukerji, T., and Nur, A., 2002 (this volume), Analysis of 3D high-resolution seismic reflection and crosswell radar tomography for aquifer characterization: A case study: Near-Surface Geophysics, v. II, Soc. Expl. Geoph., Tulsa.

Baker, G. S., Steeples, D. W., and Schmeissner, C., 1999, In-situ, high-resolution P-Wave velocity measurements within 1 m of the Earth's surface: Geophysics, **64**, 323-325.

Berge, P. A., and Bonner, B. P., 2002, Seismic velocities contain information about depth, lithology, fluid content, and microstructure: Expanded Abstracts of the Annual Symposium on the Application of Geophysics to Engineering and Environmental Problems (SAGEEP), Las Vegas, NV, February 10-14, 2002, Environmental and Engineering Geophysical Society, Wheat Ridge, CO, also submitted to the Journal of Environmental and Engineering Geophysics.

Berge, P. A., Berryman, J. G., Bonner, B. P., Roberts, J. J., and Wildenschild, D., 1999, Comparing geophysical measurements to theoretical estimates for soil mixtures at low pressures: *in* Powers, M. H., Cramer, L., and Bell, R. S., Eds., Proceedings of the 12th Annual Symposium on the Application of Geophysics to Engineering and Environmental Problems (SAGEEP), Oakland, California, March 14-18, 1999, Environmental and Engineering Geophysical Society, Wheat Ridge, CO, 465-472.

Bertete-Aguirre, H., and Berge, P. A., 2002, Recovering soil distributions from seismic data using laboratory velocity measurements: Journal of Environmental and Engineering Geophysics, 7, 1-10.

Bonner, B. P., Hart, D. J., and Berge, P.A., 1997, Influence of chemistry on physical properties: ultrasonic velocities in mixtures of sand and swelling clay (abstract): Eos,

Transactions of the American Geophysical Union, Fall Meeting Supplement, **78**, F679.

Bonner, B. P., Berge, P. A., Aracne-Ruddle, C., Boro, C., Hardy, E., and Trombino, C., 1999a, Ultrasonic characterization of synthetic soils for application to near-surface geophysics: *in* Powers, M. H., Cramer, L., and Bell, R. S., Eds., Proceedings of the 12th Annual Symposium on the Application of Geophysics to Engineering and Environmental Problems (SAGEEP), Oakland, California, March 14-18, 1999, Environmental and Engineering Geophysical Society, Wheat Ridge, CO, 455-463.

Bonner, B. P., Boro, C., and Hart, D. J., 1999b, Anti-waveguide for ultrasonic testing of granular media under elevated stress: LLNL Patent disclosure IL-10607, and patent application, DOE Patent Docket No. S-94-182, October 28, 1999.

Bonner, B. P., Wildenschild, D., Berge, P. A., Ruddle, D., and Aracne-Ruddle, C. M., 2000, Ultrasonic velocities of artificial sediments with minimal overburden: Eos, Transactions of the American Geophysical Union, Fall Meeting Supplement, Proceedings of the Fall Annual Meeting, San Francisco, CA, Dec. 15-19, 2000, **81**, F1105.

Bonner, B. P., Berge, P. A., and Wildenschild, D., 2001, Compressional and shear wave velocities for artificial granular media under simulated near surface conditions Expanded abstract, Society of Exploration Geophysicists International Exposition and Seventy-First Annual Meeting, Sept. 9-14, 2001, San Antonio, TX.

Boulanger, R. W., Arulnathan, R., Harder, L. F., Jr., Torres, R. A., and Driller, M. W., 1998, Dynamic properties of Sherman Island peat: ASCE Journal of Geotechnical and Geoenvironmental Engineering, **124**, 12-20.

Carr, B. J., Hajnal, Z., and Prugger, A., 1998, Shear-wave studies in glacial till: Geophysics, **63**, 1273-1284.

Cheng, C. H., 1978, Seismic velocities in porous rocks: direct and inverse problems: Ph.D. thesis, Mass. Inst. of Technol., Cambridge, Mass.

Crouse, C. B., Kramer, S. L., Mitchell, R., and Hushmand, B., 1993, Dynamic tests of pipe pile in saturated peat: ASCE Journal of Geotechnical Engineering **119**, 1550-1567.

Domaschuk, L., and Wade, N. H., 1969, A study of bulk and shear moduli of a sand: J. Soil Mech. Found. Div., Proc. ASCE, **95**, 561-581.

Domenico, S. N., 1976, Effect of brine-gas mixture on velocity in an unconsolidated sand reservoir: Geophysics, **41**, 882-894.

Futterman, W. I., 1962, Dispersive body waves: JGR, **67**, 5279-5291.

Gassmann, F., 1951, Über die elastizität poröser medien: Vierteljahrsschrift der Naturforschenden Gesellschaft in Zürich, **96**, 1-23.

Green, D. H., Wang, H. F., and Bonner, B. P., 1993, Shear wave attenuation in dry and saturated sandstone at seismic to ultrasonic frequencies: Int. J. Rock Mech. Min. Sci. & Geomech. Abstr. **30**, 755-761.

Hamilton, E. L., and Bachman, R. T., 1982, Sound velocity and related properties of marine sediments: J. Acoust. Soc. Am., **72**, 1891-1904.

Han, D., Nur, A. and Morgan, F. D., 1986, Effect of porosity and clay content on wave velocities of sandstones: Geophysics, **51**, 2093-2107.

Hübner, S., Meissner, R., and Stümpel, H., 1985, Einflüsse lithologischer Parameter oberflächennaher Sedimente auf Kompressions- und Scherwellengeschwindigkeiten: *in* Ingenieurgeologische Probleme in Grenzbereich zwischen Locker- und Festgesteinen, Springer-Verlag, Berlin, 583-596.

Knight, R., and Nolen-Hoeksema, R., 1990, A laboratory study of the dependence of elastic wave velocities on pore scale fluid distribution: Geophys. Res. Lett. **17**, 1529-1532.

Kuster, G. T., and M. N. Toksöz, 1974, Velocity and attenuation of seismic waves in two-phase media, Part I, Theoretical formulations, and Part II, Experimental results: Geophysics **39**, 587-618.

Marion, D., Nur, A., Yin, H., and Han, D., 1992, Compressional velocity and porosity in sand-clay mixtures: Geophysics, **57**, 554-563.

OConnell, R. J., and Budiansky, B., 1977, Viscoelastic properties of fluid-saturated cracked solids: JGR, **82**, no. 36, 5719-5735.

Palciauskas, V. V., 1992, Compressional to shear wave velocity ratios of granular rocks: role of rough grain contacts: GRL, **19**, no.16, 1683-1686.

Prasad, M., 2002, Acoustic measurements in sands at low effective pressure: Overpressure detection in sands: Geophysics, **67**, no. 2, 405 – 412.

Prasad, M., and Manghnani, M. H., 1997, Effects of pore and differential pressures on compressional wave velocity and quality factor on Berea and Michigan sandstones: Geophysics, **62**, no. 4, 1163-1176.

Prasad M., and Meissner, R., 1992, Attenuation mechanisms in sands: Laboratory versus theoretical (Biot) data: Geophysics, **57**, no. 5, 710-719.

Rao, H. A. B., 1966, Wave velocities through partially saturated sand-clay mixtures: Response of Soils to Dynamic Loadings Report 24, Mass. Inst. Tech. Dept. Civ. Eng. Research Report R66-13, Soils Pub. 194, Defense Documentation Center, Cameron Station, Alexandria, VA.

Robertson, P. K., S. Sasitharan, J. C. Cunning, and D. C. Sego, 1995, Shear-wave velocity to evaluate in-situ state of Ottawa Sand: J. Geotech. Eng., **121,** 262-273.

Santamarina, J.C., Klein, K.A., and Fam, M.A., 2001, Soils and Waves: John Wiley and Sons, West Sussex, England.

Sears, F. M., and Bonner, B. P., 1981, Ultrasonic attenuation measurement by spectral ratios utilizing signal processing techniques: IEEE Transactions on Geoscience and Remote Sensing, **GE-19**, 95-99.

Steeples, D. W., Baker, G. S., and Schmeissner, C., and Macy, B. K., 1999, Geophones on a board: Geophysics, **64**, no. 3, 809-814.

Taylor, W. P., and Wilson, C. D. V., 1997, Tectonically influenced glacial erosion, and ensuing valley infill: A geophysical survey: Quarterly Journal of Engineering Geology **30**, 97-113.

Vernik, L., and Nur, A., 1992, Petrophysical classification of siliciclastics for lithology and porosity prediction from seismic velocities: Am. Assoc. Petr. Geol. Bull. **76**, 1295-1309.

Wilkens, R. H., Simmons, G., Wissler, T. M., and Caruso, L., 1986, The physical properties of a set of sandstones--Part III. The effects of fine-grained pore-filling material on compressional wave velocity: Int. J. Rock Mech. Min. Sci. & Geomech. Abstr. **23**, 313-326.

Winkler, K. W., 1983, Contact stiffness in granular porous materials. Comparison between theory and experiments: Geophy. Res. Lett., **10**, 1073-1076.

Winkler, K. W., and Nur, 1982, Seismic attenuation: Effects of pore fluids and frictional sliding: Geophysics, **47, no.** 1, 1-15.

Wyllie, M. R. J., Gregory, A. R., and Gardner, L. W., 1956, Elastic wave velocities in heterogeneous and porous media: Geophysics, **21**, 41-70.

Yin, H., 1992, Acoustic velocity and attenuation of rocks: isotropy, intrinsic anisotropy, and stress induced anisotropy: Ph.D. thesis, Stanford Univ.

Zimmer, M. A., Prasad, M., and Nur, A., 2000, Ultrasonic velocities of sand at low effective pressures (abstract): Eos, Transactions of the American Geophysical Union, Fall Meeting Supplement, Proceedings of the Fall Annual Meeting, held in San Francisco, CA, Dec. 15-19, 2000, **81**, F1105-1106.

Zimmer, M. A., Prasad, M., and Nur, A., 2002a, Laboratory P- and S-wave measurements on sands: Implications for pressure trends: Expanded Abstracts of the Annual Symposium on the Application of Geophysics to Engineering and Environmental Problems (SAGEEP), Las Vegas, NV, February 9-13, 2002, Environmental and Engineering Geophysical Society, Wheat Ridge, CO.

Zimmer, M., Prasad, M., and Mavko, G., 2002b, Pressure and porosity influences on Vp-Vs ratio in unconsolidated sands: The Leading Edge, **21**, no. 2, 178-183.

FIGURE CAPTIONS

Fig. 1. Schematic diagram of pore fluid pumping system for LLNL apparatus.

Fig. 2. (a) The Stanford sample holder. (b) The Stanford pressure vessel in its stand.

Fig. 3. Typical signals from the Stanford experiment. P-wave signals in a sand sample are shown in (a) at 0.05 MPa and (b) at 20 MPa confining pressures. S-wave signals in a sand sample are shown in (c) at 0.05 MPa and (d) at 20 MPa confining pressures. Arrows in (c) and in (d) mark onset of the S-wave.

Fig. 4. (a) Vp and (b) Vs versus pressure for various sand-clay mixtures. Numbers in legend of plot refer to date of measurement and clay content (by mass) for sand-clay mixtures. Different samples had different packing in some cases. (1 MPa = 145 psi).

Fig. 4. (c) (top) Velocity vs. clay content for dry sand-clay mixtures at 16 psi (0.11 MPa) and (bottom) schematic diagram of microstructure for various amounts of clay (black) mixed with sand grains (gray circles).

Fig. 5. Ultrasonic velocity results for dry and water-saturated samples of the Santa Cruz aggregate. (a) Vp and (b) Vs for the four sand samples.

Figure 6. Separation of saturation effects using a loss diagram (Prasad and Meissner, 1992). Water-saturated sands (filled circles) are characterized by high Vp/Vs and Qp/Qs values, whereas dry sands (open triangles) have low Vp/Vs values but high Qp/Qs. The solid lines are calculations for various values of bulk (K_i) and shear (μ_i) losses. Shear losses are as high as bulk losses in dry sands whereas in saturated sands, shear losses are higher. Vp/Vs and Qp/Qs values decrease with confining pressure as marked by arrows (data from Prasad and Meissner, 1992; and Prasad, 2002).

Figure 7. A typical shallow soil scenario in a clean sand environment and the Vp, Vs, Vp/Vs profile of such a sediment packet. The water-table is clearly marked by high Vp/Vs ratios that decrease with depth. In the dry and the partially saturated zones, Vp/Vs values are low and they do not change much with pressure. In all cases, velocity is strongly dependent on depth.

LIST OF TABLES

Table 1. LLNL velocity results for partially-saturated sand samples at 40 kPa load.

Table 2. Empirical fits to the velocity data for Santa Cruz aggregate samples (between 0.1 and 20 MPa).

Table 3. Poisson's ratios for dry samples at low pressures.

Table 4. Poisson's ratios for dry and saturated samples at hydrostatic pressures.

FIGURES

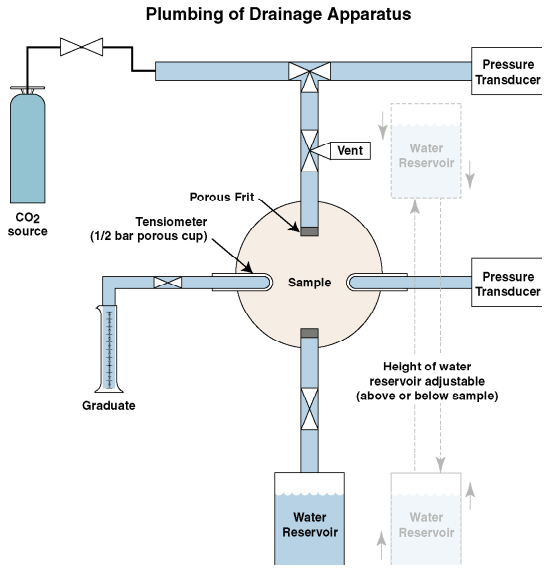

Fig. 1. Schematic diagram of pore fluid pumping system for LLNL apparatus.

(a) (b)

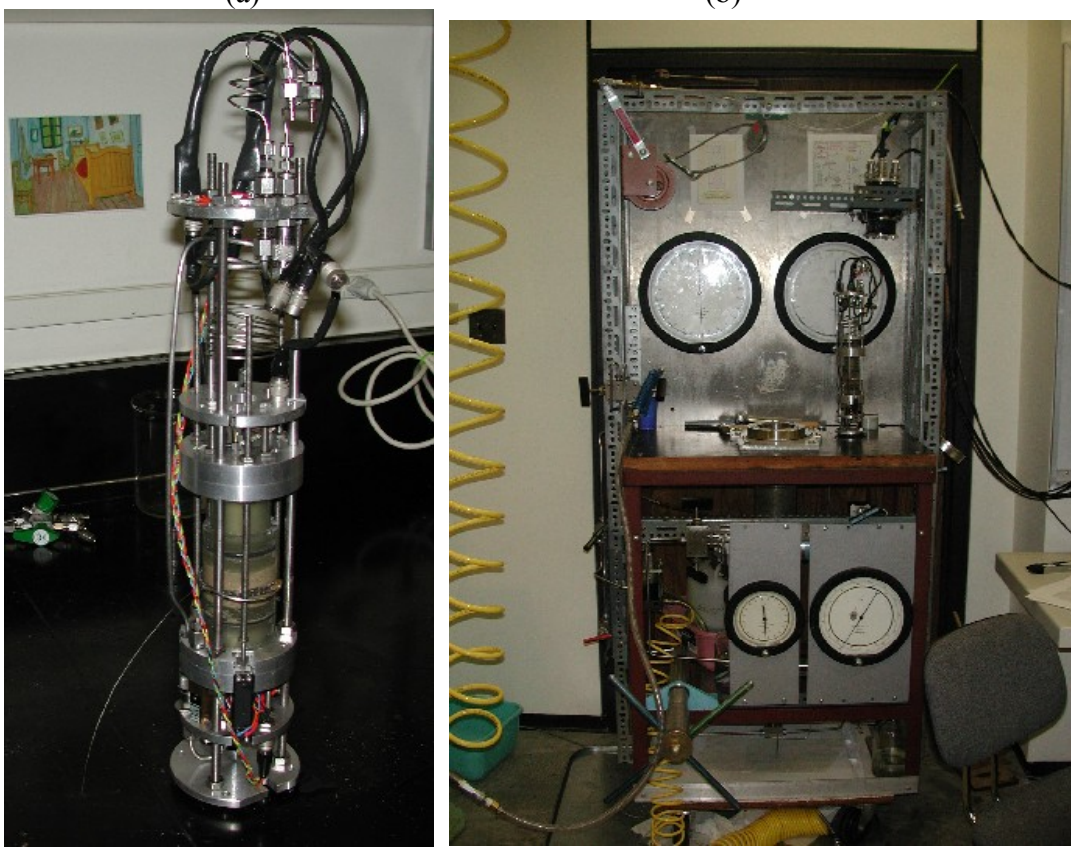

Fig. 2. (a) The Stanford sample holder. (b) The Stanford pressure vessel in its stand.

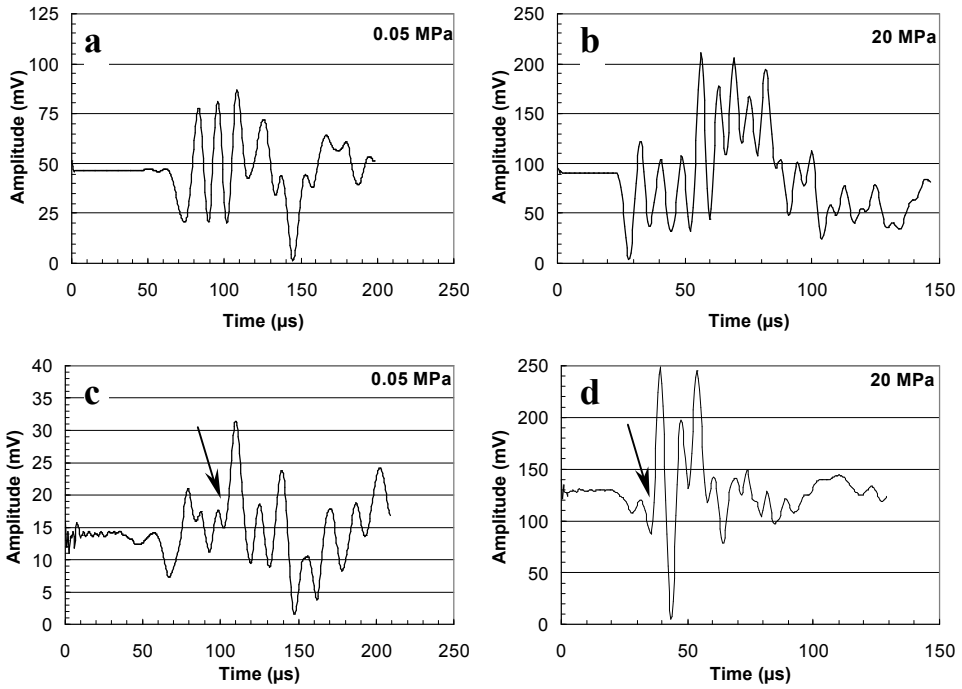

Fig. 3. Typical signals from the Stanford experiment. P-wave signals in a sand sample are shown in (a) at 0.05 MPa and (b) at 20 MPa confining pressures. S-wave signals in a sand sample are shown in (c) at 0.05 MPa and (d) at 20 MPa confining pressures. Arrows in (c) and in (d) mark onset of the S-wave.

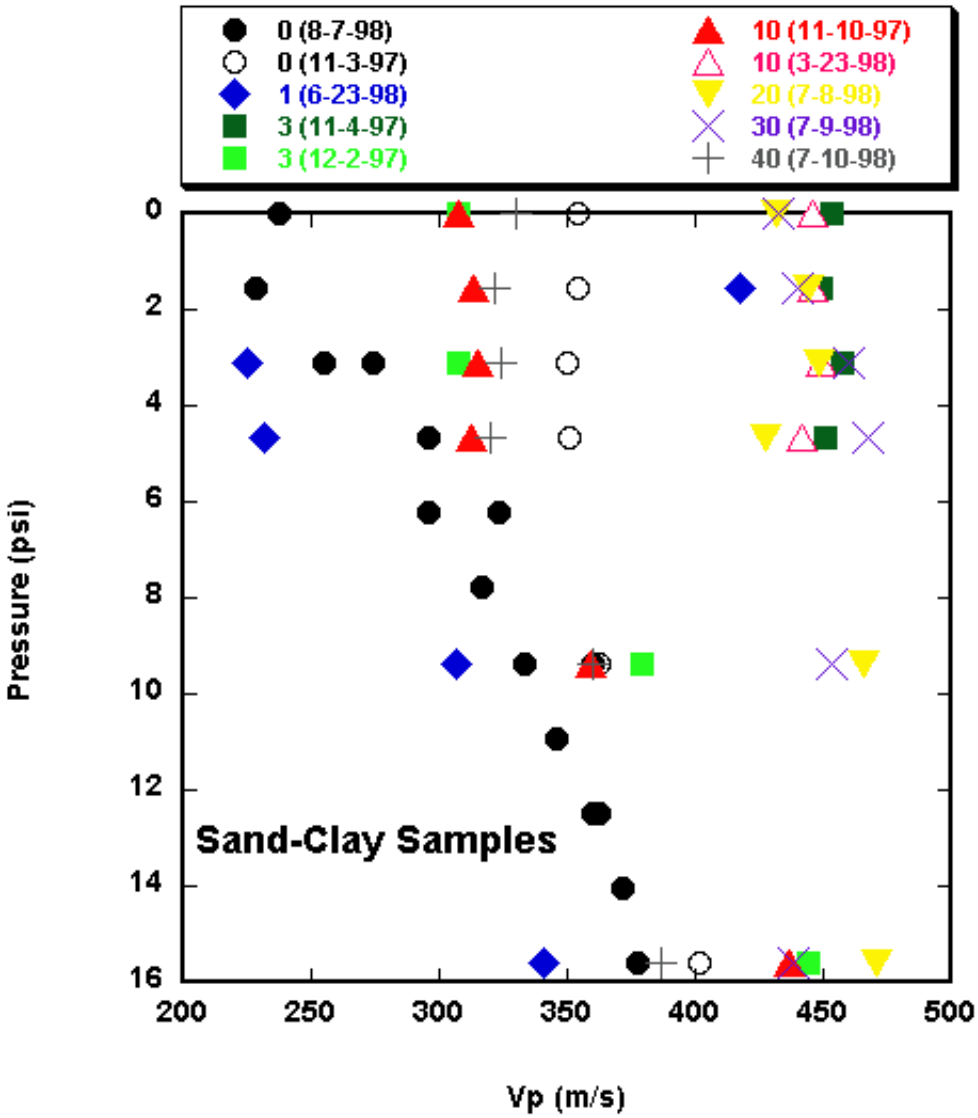

Fig. 4. (a) Vp vs. pressure for various sand-clay mixtures. Numbers in legend of plot refer to date of measurement and clay content (by mass) for sand-clay mixtures. Different samples had different packing in some cases. (1 MPa = 145 psi)

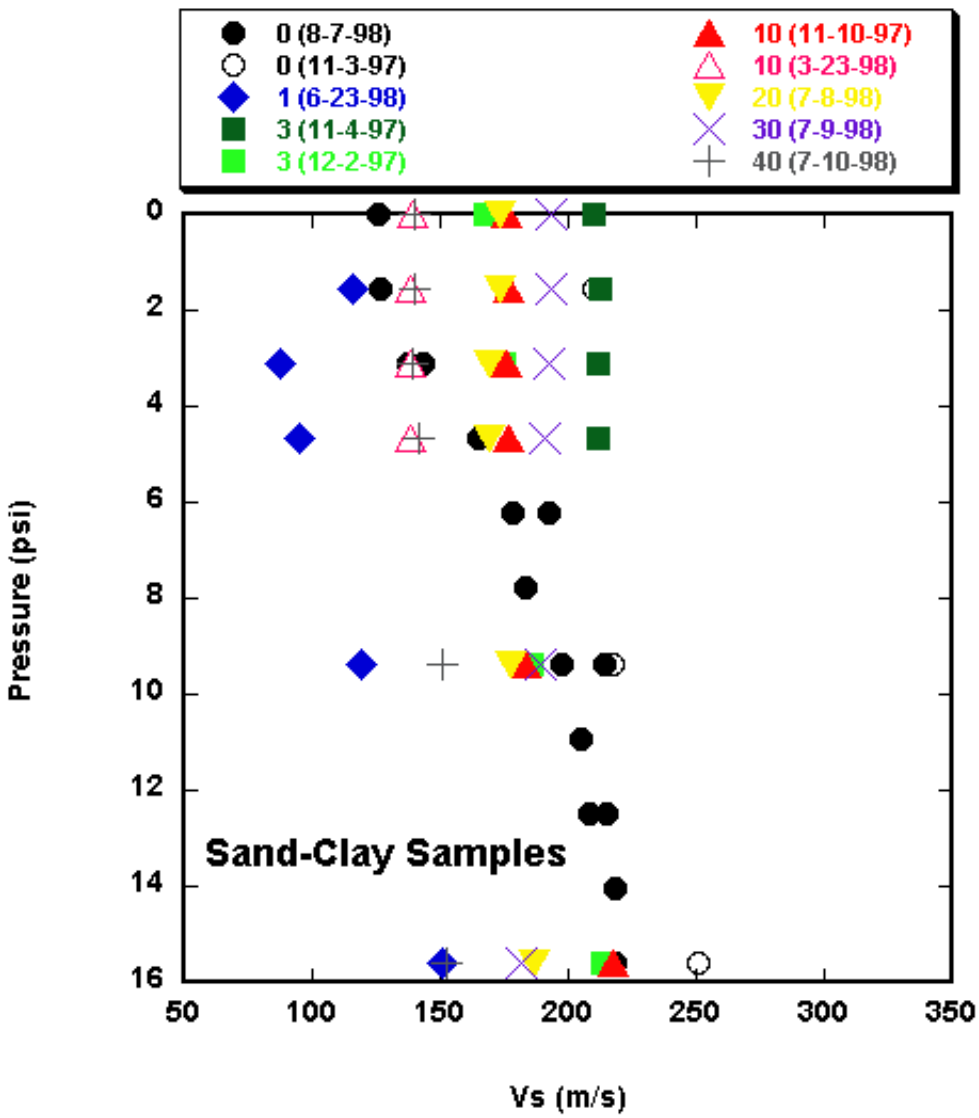

Fig. 4. (b) Vs versus pressure for various sand-clay mixtures. Numbers in legend of plot refer to date of measurement and clay content (by mass) for sand-clay mixtures. Different samples had different packing in some cases. (1 MPa = 145 psi)

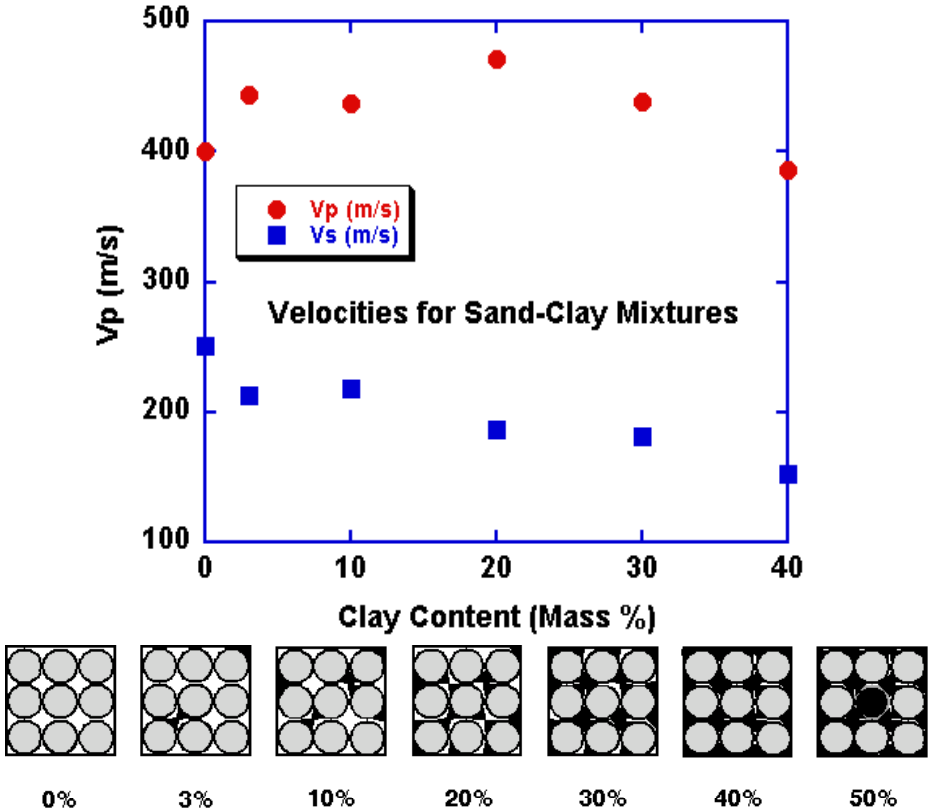

Fig. 4. (c) (top) Velocity vs. clay content for dry sand-clay mixtures at 16 psi (0.11 MPa) and (bottom) schematic diagram of microstructure for various amounts of clay (black) mixed with sand grains (gray circles).

(a) P-waves

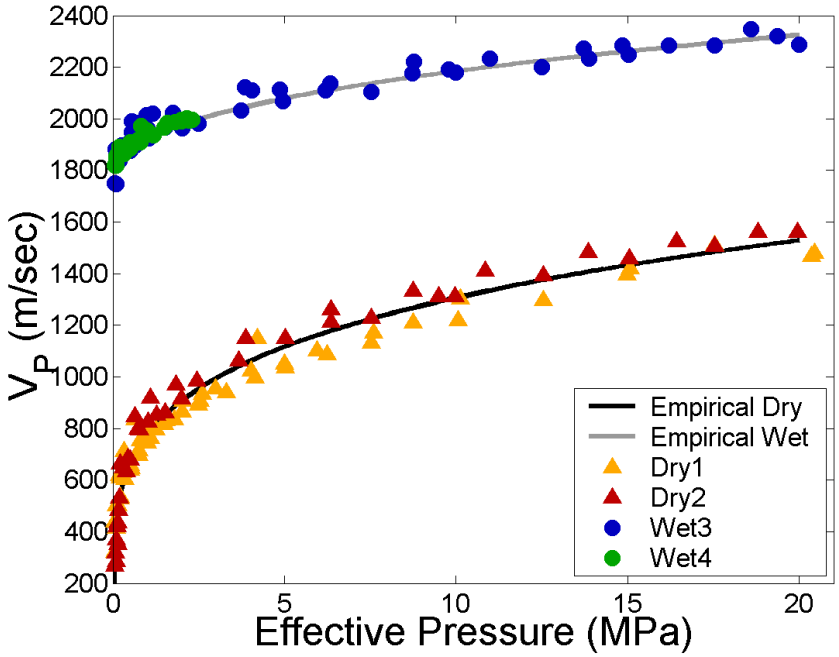

(b) S-waves

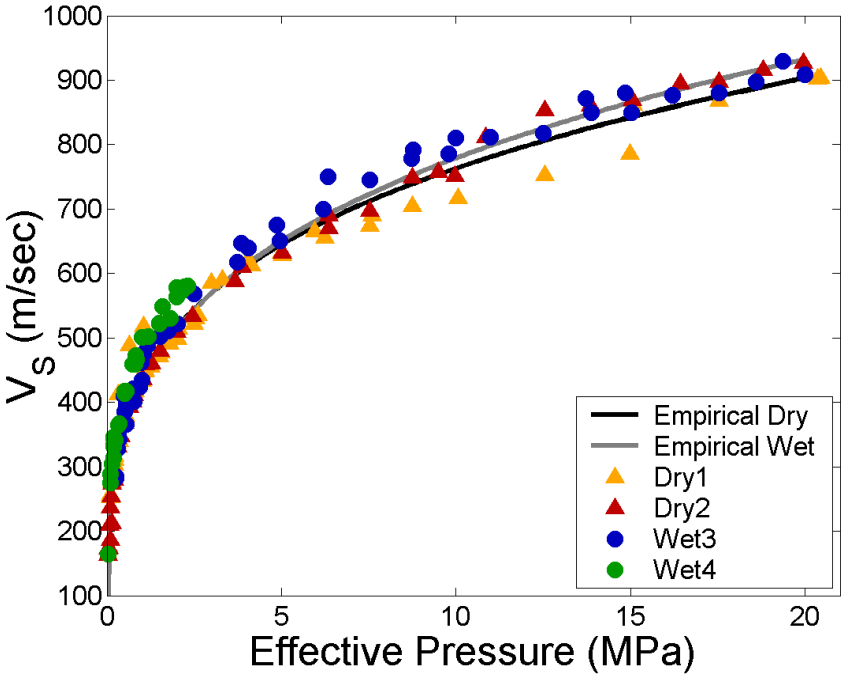

Fig. 5. Ultrasonic velocity results for dry and water-saturated samples of the Santa Cruz aggregate. (a) Vp and (b) Vs for the four sand samples.

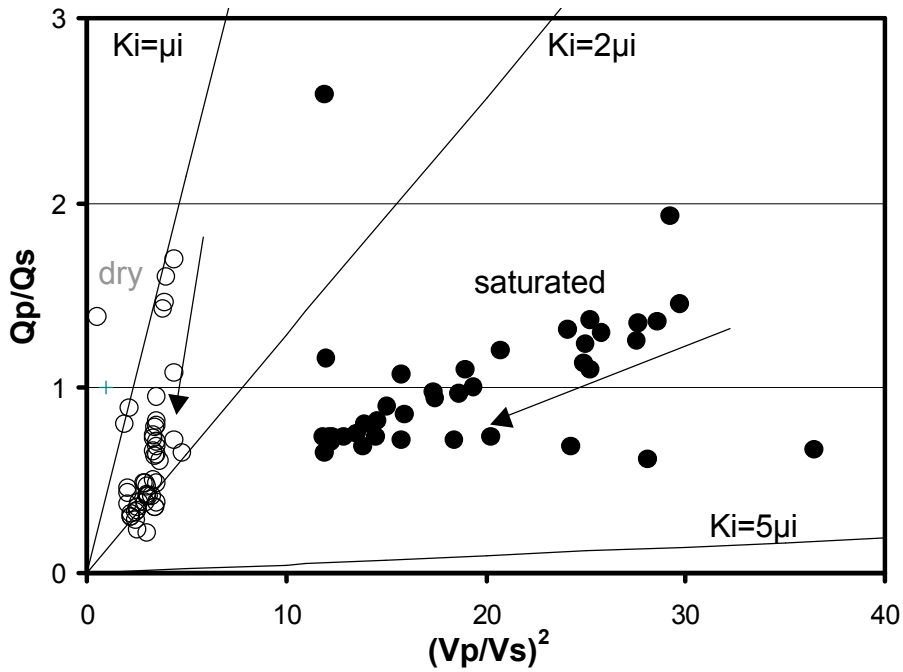

Figure 6. Separation of saturation effects using a loss diagram (Prasad and Meissner, 1992). Water-saturated sands (filled circles) are characterized by high Vp/Vs and Qp/Qs values, whereas dry sands (open triangles) have low Vp/Vs values but high Qp/Qs. The solid lines are calculations for various values of bulk (K_i) and shear (μ_i) losses. Shear losses are as high as bulk losses in dry sands whereas in saturated sands, shear losses are higher. Vp/Vs and Qp/Qs values decrease with confining pressure as marked by arrows (data from Prasad and Meissner, 1992; and Prasad, 2002).

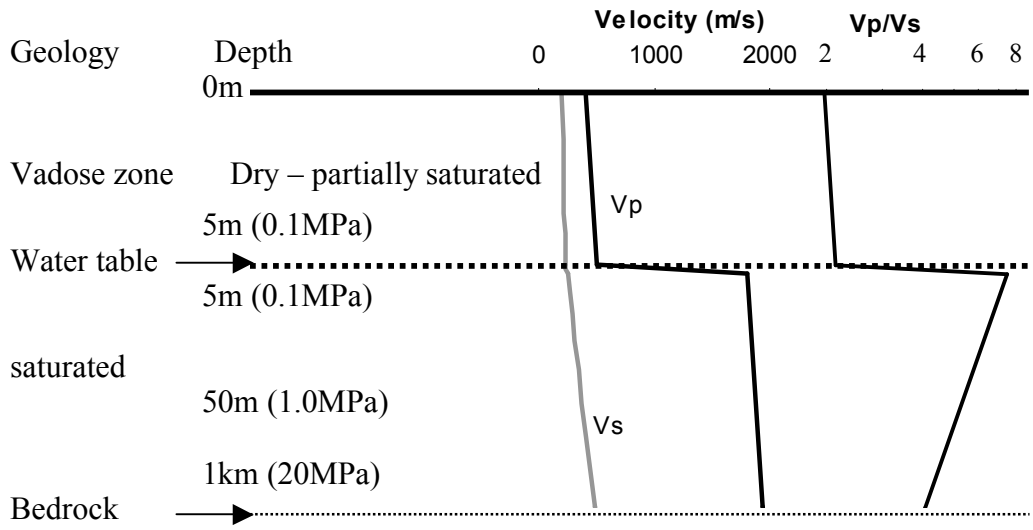

Figure 7. A typical shallow soil scenario in a clean sand environment and the Vp, Vs, Vp/Vs profile of such a sediment packet. The water-table is clearly marked by high Vp/Vs ratios that decrease with depth. In the dry and the partially saturated zones, Vp/Vs values are low and they do not change much with pressure. In all cases, velocity is strongly dependent on depth.

TABLES

Table 1. LLNL velocity results for partially-saturated sand samples at 40 kPa load

Waveform	Vp (m/s)	Vs (m/s)	Poisson's ratio	Notes
Sample 1:				
6/27/00 #1	375 ± 75	232 ± 6	0.19	Saturated, but some bubbles. (Vp =1500 ± 40 through sat. patches)
Sample A:				
6/29/00 #2	357 ± 30	214 ± 10	0.22	Saturated, no visible bubbles
6/30/00 #1	308 ± 10	214 ± 10	0.03	Draining (capillary press = 35 cm), water content 22 to 28 %.
6/30/00 #3	326 ± 10	204 ± 6	0.18	Draining (capillary press = 44 cm), water content 13 to 17 %.
12/7/00	349 ± 8	249 ± 20	~0	Dried (chemical alteration probable)

Table 2. Empirical fits to the velocity data for Santa Cruz aggregate samples (between 0.1 and 20 MPa).

	a	b	c	1/c (root)	R^2
V_S – dry	0	436	0.243	4.11	0.9852
V_S – wet	0	428	0.260	3.84	0.9572
V_P – dry	0	774	0.227	4.40	0.9656
V_P – wet	1753	168	0.408	2.45	0.9295

Table 3. Poisson's ratios for dry samples at low pressures.

Clay content	Pressure	Vp/Vs	Poisson's ratio
0%	~0 MPa	1.7 - 2.2	0.23 - 0.36
0%	~0.1 MPa	1.6 - 2.1	0.18 - 0.36
1%	~0 MPa	3.6	0.46
1%	~0.1 MPa	2.3	0.38
3%	~0 MPa	1.8 - 2.2	0.29 - 0.36
3%	~0.1 MPa	2.1 - 2.2	0.35 - 0.37
10%	~0 MPa	1.8 - 3.2	0.26 - 0.45
10%	~0.1 MPa	2.0 - 3.2	0.33 - 0.45
20%	~0 MPa	2.5	0.4
20%	~0.1 MPa	2.5	0.41
30%	~0 MPa	2.2	0.38
30%	~0.1 MPa	2.4	0.4
40%	~0 MPa	2.4	0.39
40%	~0.1 MPa	2.5	0.41

Table 4. Poisson's ratios for dry and saturated samples at hydrostatic pressures.

DRY				
Pressure (MPa)	Vp (m/s)	Vs (m/s)	Vp/Vs	Poisson's ratio
0.0	275	160	1.72	0.24
0.101	501	235	2.13	0.36
0.15	500	268	1.87	0.30
0.201	510	290	1.76	0.26
0.3	549	330	1.66	0.22
0.5	640	365	1.75	0.26
1.02	821	434	1.89	0.31
2.46	982	534	1.84	0.29
5.03	1131	631	1.79	0.27
7.52	1225	697	1.76	0.26
9.97	1309	750	1.75	0.26
15.05	1445	861	1.68	0.22
17.54	1504	895	1.68	0.23
19.96	1566	925	1.69	0.23
SATURATED				
0.111	1810	244	7.42	0.49
0.2	1836	271	6.77	0.49
0.292	1877	338	5.53	0.48
0.5	1883	378	4.87	0.48
1.049	1938	477	4.05	0.47
2.499	1973	569	3.48	0.45
4.947	2062	651	3.18	0.44
7.52	2108	752	2.83	0.43
9.792	2180	786	2.79	0.43
15.017	2246	850	2.65	0.42
17.526	2285	880	2.60	0.41
19.992	2286	908	2.52	0.41